Signatures of Planets in Protoplanetary and Debris Disks

Sebastian Wolf [a], Amaya Moro-Martín [b], Gennaro D'Angelo [c,d]

[a] *Max Planck Institute for Astronomy, Königstuhl 17, 69117 Heidelberg, Germany; swolf@mpia.de*

[b] *Department of Astrophysical Sciences, Peyton Hall, Ivy Lane, Princeton University, Princeton, NJ 08544, USA; amaya@astro.princeton.edu*

[c] *School of Physics, University of Exeter, Stocker Road, Exeter EX4 4QL, UK; gennaro@astro.ex.ac.uk*

[d] *NASA Ames Research Center, Space Science and Astrobiology Division, MS 245-3, Moffett Field, CA 94035, USA*

Abstract

We discuss selected possibilities to detect planets in circumstellar disks. We consider the search for characteristic signatures in these disks caused by the interaction of giant planets with the disk as the most promising approach. Numerical simulations show that these signatures are usually much larger in size than the planet itself and thus much easier to detect. The particular result of the planet-disk interaction depends on the evolutionary stage of the disk. Primary signatures of planets embedded in disks are gaps in the case of young disks and characteristic asymmetric density patterns in debris disks.

We present simulations which demonstrate that high spatial resolution observations performed with instruments / telescopes that will become available in the near future will be able to trace the location and other properties of young and evolved planets. These observations will allow to directly investigate the formation and evolution of planets in protoplanetary and debris disks.

Key words: Protoplanetary disk, Debris disk, Planet formation, Planet-disk-interaction, Radiative transfer simulation

1 Introduction

Planets are expected to form in circumstellar disks, which are considered as the natural outcome of the protostellar evolution, at least in the case of low and intermediate mass stars (e.g., Adams et al. 1987; Lissauer 1993). While a detailed picture of the evolution of the circumstellar environment, in particular of circumstellar disks, has been developed already, the planet formation process is in major parts still under discussion. In particular, adequate constraints from observations are required in order to either verify or rule out currently discussed planet formation scenarios (e.g., Pollack et al. 1996, Weidenschilling 1997, Goldreich & Ward 1973, Youdin & Shu 2002).

Although many extra-solar planet candidates have been detected indirectly by radial velocity variations of stars (e.g., review by Marcy et al. 2005) no firm direct imaging detection of a planet has been obtained so far. The main difficulty is the large brightness contrast between a star and a planet combined with their small angular distance. One can try to avoid this problem for example by searching for planetary companions around nearby stars, making use of high-resolution imaging techniques, nulling interferometry, or coronagraphy. Furthermore, the brightness ratio between the star and the presumed planetary companion can be decreased by choosing a proper wavelength range, spectral type of the star, and age / evolutionary stage of the planet (e.g., Hubbard et al. 2002).

Finding and imaging planets which are *still embedded* in a circumstellar disk is by far more difficult, because the dust continuum radiation dominates the whole spectral range from the ultraviolet to millimeter wavelengths: In the ultraviolet to the near-infrared by scattering of the stellar radiation and at longer wavelengths by thermal reemission. Thus, in the preparation of observations of planets in disks even more constraints have to be taken into account, describing the properties of the disk, such as the optical parameters of the dust (chemical composition, size distribution) and its spatial temperature and density distribution. In the case of young, optically thick circumstellar disks, the disk inclination and possible accretion on the planet have to be considered as well.

Despite these obvious problems to investigate planets during the final stages of their formation or early evolution through direct imaging, the following approach is currently under discussion. During recent years, numerical simulations **and analytical studies** of planet-disk interactions have shown that planets may cause characteristic large-scale signatures in the density distribution of circumstellar disks. The most important of these signatures are gaps and spiral density waves in young, also called "protoplanetary" disks and resonance structures in evolved systems, so-called "debris disks". The importance

of investigating these signatures lies in the possibility to use them in the search for embedded planets. Therefore, disk features can provide constraints on the processes and timescales of planet formation.

In the following sections we discuss characteristic signatures in circumstellar disks caused by the planetary perturbation. Moreover, we focus on the question whether these signatures could be observed and thus be used as tracers for planets and the physical conditions in their close vicinity. In Sect. 2 we consider protoplanetary disks, and in Sect. 3 debris disks. This distinction is helpful since the main physical processes dominating the structure of a disk with an embedded planet are different in both cases, resulting in different characteristic features.

2 Protoplanetary Disks

Protoplanetary disks are accretion disks which have been found around T Tauri and Herbig Ae/Be stars. Hydrodynamic simulations of gaseous, viscous protoplanetary disks with an embedded protoplanet show that planets with masses

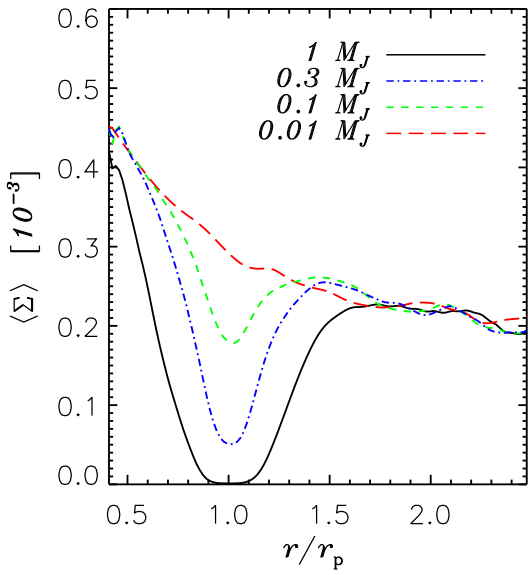

Fig. 1. Azimuthally averaged disk surface density $\langle\Sigma\rangle$ for planets with masses from 0.01 to 1 $M_{Jupiter}$, around a solar-mass star (r_P is the radius of the planetary orbit). In physical units, $\langle\Sigma\rangle = 10^{-4}$ corresponds to $33\,g\,cm^{-2}$. The depth and width of the density gap depend mainly on the planet's mass (as the plot indicates), the disk temperature, and the viscosity of the disk material. Notice that, in a cold disk with low viscosity also a planet with a mass of a few times 10 M_{Earth} could open a deep gap.

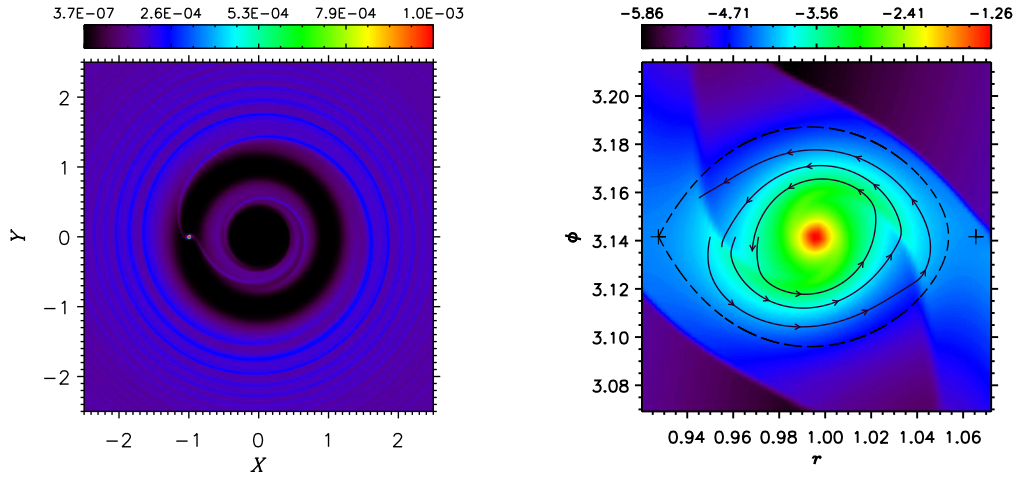

Fig. 2. [Left] Surface density of a **circumstellar** disk with an embedded 1 $M_{Jupiter}$ planet, which shows the planet, the gap, and the spiral-wave pattern excited by the planet. [Right] Density in the planet's Roche lobe that shows the circumplanetary disk (with selected streamlines), i.e., the disk around the planet. The density scale on top of each panel is linear (left) and logarithmic (right). The physical units are as in Figure 1.

$\gtrsim 0.1\,M_{Jupiter}$ produce significant perturbations in the disk's surface density. In particular, they may open and maintain a large gap as illustrated in Figure 1. (e.g., Bryden et al. 1999; Kley 1999; D'Angelo et al. 2002 ; Bate et al. 2003). This gap, which is located along the orbit of the planet, may extend up to several astronomical units in width, depending on the mass of the planet and the hydrodynamic properties of the disk (see caption of Fig. 1 for further details). Nevertheless, the disk mass **flow onto** the planet continues through the gap with high efficiency. **Nearly all of the flow through the gap is accreted by the planet at a rate comparable to the rate at which mass accretion would occur in the disk without a planet.** The gas accretion on the planet can continue to planet masses of the order of $10\,M_{Jupiter}$, at which point tidal forces are sufficiently strong to prevent flow into the gap. However, planets with final masses of the order of $1\,M_{Jupiter}$ would undergo migration on a timescale of about 10^5 years, which could make survival difficult.

Protoplanets also launch spiral waves in the disk (see Fig. 2[left]). However, in the presence of turbulence, these waves appear to be diffused (Nelson & Papaloizou 2003). Furthermore, D'Angelo et al. (2002) found smaller-scale spirals in the vicinity of the planet that are detached from the main ones: Along these small spirals the gas orbits the planet, forming a circumplanetary disk (see Fig. 2[right]; see also Lubow et al. 1999).

The observability of the features outlined above has been first investigated by Wolf et al. (2002). It was shown that high-resolution images in the submillimeter wavelength range, as to be obtained with the *Atacama Large Millimeter*

Array[1] (*ALMA*), will allow to trace the gap but not the large-scale spiral structure.

We perform further simulations with the goal of answering the question whether the planet *itself* and/or the circumplanetary environment heated by the planet, through its contraction and/or via accretion onto it, could be detected. The detection of a gap would already represent a strong indication of the existence of a planet, thus giving information such as planetary mass, disk viscosity, and pressure scale-height of the disk. The detection / non-detection of warm dust close to the planet, however, would additionally provide valuable constraints on the temperature and luminosity of the planet, the accretion process, and the density structure of the surrounding medium.

This study is motivated also by the assumption that young giant planets are expected to be very hot, compared to their old counterparts, such as Jupiter. Even more importantly, the accretion onto the planet is expected to release enough energy to sufficiently heat the circumplanetary environment. Thus, the planet surroundings might be observable in the (far-)infrared wavelength range through thermal dust reemission. Provided that the mass of the planet is large enough to open a significantly large and low-density gap (on the order of a Jupiter's mass), the contrast between the gap and the dust heated by the planet might be sufficiently high to allow one to distinguish both components, i.e., the gap and the dust distribution around the planet.

We test different environments of a planet located in a circumstellar disk for the resulting temperature structure which, in combination with the density distribution, mainly determines the likelihood to detect any of the features characterizing the embedded planet. The models considered here cover a broad range of different, most reasonable scenarios. A detailed description of all considered model configurations and the resulting observational consequences is given in Wolf & D'Angelo (2005). In the following, we concentrate on the most significant results of this study.

2.1 The planetary accretion region as a hotspot in a young **disk**

The evolution of a circumstellar disk with an embedded planet can be formally described by the Navier-Stokes equations for the density and the velocity field components (see, e.g., D'Angelo et al. 2002 for details). For the purpose of the present study, the disk is treated as a two-dimensional viscous fluid in the equatorial plane. Disk material is supposed to have a constant kinematic viscosity that is equivalent to a Shakura & Sunyaev parameter $\alpha = 4 \times 10^{-3}$ at the location of the planet.

[1] see, e.g., http://www.alma.nrao.edu/

A planet-sized object with mass $M_{\rm P}$ revolves around the central star, moving on a circular orbit whose radius is $r_{\rm P}$. It perturbs the surrounding environment via its point-mass gravitational potential. The ratio of $M_{\rm P}$ to M_* is 2×10^{-3}, hence $M_{\rm P} = 1\,{\rm M_{jup}}$ if $M_* = 0.5\,{\rm M_{sun}}$. We base this study on two-dimensional models because, by means of high-resolution three-dimensional simulations, D'Angelo et al. (2003) demonstrated that computations in two dimensions give a satisfactory description of disk-planet interactions when dealing with heavy planets ($M_{\rm P}/M_* > 10^{-4}$) in thin disks (aspect-ratio ≈ 0.05).

The simulations are started from a purely Keplerian disk. Due to the angular momentum transfer among the inner disk ($r < r_{\rm P}$), the planet, and the outer disk ($r > r_{\rm P}$), a deep density gap is soon carved in along the orbital path. Characteristic spiral features, spreading both interior and exterior to the planet's orbit are excited by the gravitational potential of the planet (Fig. 2, left panel). The disk depletion interior to the planet's orbit ($r < r_{\rm P}$), due both to gravitational torques exerted by the planet on the disk material and to viscous diffusion towards the star, is accounted for by allowing material to flow out of the inner border of the simulated disk domain, thus accounting for accretion onto the central star. These calculations also simulate the growth rate of the planet due to the feeding process by its surroundings. A fraction of the matter orbiting the planet inside of an accretion region is removed on a timescale on the order of a tenth of the orbital period. Since the accretion process is a highly localized phenomenon, the accretion region must be small. Therefore, we choose a radius $r_{\rm P}^{\rm acc}$ equal to $6 \times 10^{-2}\,r_{\rm H}$, where the Hill radius $r_{\rm H} = r_{\rm P}\,\sqrt[3]{M_{\rm P}/(3\,M_*)} = 8.7 \times 10^{-2}\,r_{\rm P}$ approximately characterizes the sphere of gravitational influence of the planet. In order to achieve the necessary resolution to study the flow dynamics on these short length scales, without neglecting the global circulation within the disk, we utilized a nested-grid technique (D'Angelo et al. 2002, 2003). We obtain a planetary accretion rate, $\dot{M}_{\rm P}$, on the order of $10^{-9}{\rm M_{sun}\,yr^{-1}}$.

Since a measure of the planetary accretion rate is available through our simulations, it is possible to evaluate the accretion luminosity of the planet $L^{\rm acc}$. For a planet with **a radius of a few Jupiter radii (e.g., Burrows et al. 1997),** $M_{\rm P} = 1\,{\rm M_{jup}}$ (orbiting a $M_* = 0.5\,{\rm M_{sun}}$ star) and $r_{\rm P} = 5\,{\rm AU}$, we get $L^{\rm acc} \approx 10^{-4}\,{\rm L_{sun}}$. However, the accretion rate is observed to slowly diminish with time, due to the depletion of the disk and the deepening of the gap. Hence, the accretion luminosity decays with the time. As an example, extrapolating $\dot{M}_{\rm P}$ after a few 10^4 years, the above estimate of $L^{\rm acc}$ becomes $\approx 10^{-5}\,{\rm L_{sun}}$. This value for the planetary accretion luminosity is on the same order of magnitude as the luminosity derived by **Burrows et al. (1997)** for a young Jupiter-mass planet.

Based on the density structure obtained from the hydrodynamical simulations we derive a self-consistent temperature structure in the disk. For this pur-

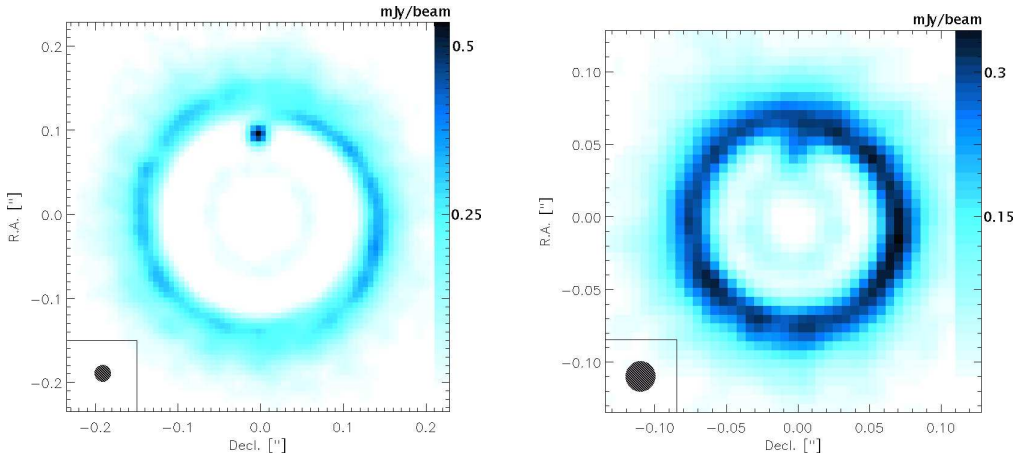

Fig. 3. Simulation of *ALMA* observations of a disk with an embedded planet with a mass of $1\,M_{jup}$ around a $0.5\,M_{sun}$ star (orbital radius: 5 AU). The assumed distance is 50 pc (left) / 100 pc (right). The disk mass amounts to $M_{disk} = 1.0 \times 10^{-2}\,M_{sun}$. Only structures above the 2σ-level are shown. The size of the combined beam is symbolized in the lower left edge of each image. Note the reproduced shape of the spiral wave near the planet and the slightly shadowed region behind the planet in the left image. *[from Wolf & D'Angelo 2005]*

pose we use the three-dimensional continuum radiative transfer code MC3D (Wolf 2003; see also Wolf et al. 1999). We derive the disk temperature structure resulting from stellar heating on a global grid covering the whole disk, but simulate the additional heating due to the planet on a much smaller grid centered on the planet, which sufficiently resolves the temperature gradient in its vicinity.

We now discuss observable quantities under the assumption that the disk is seen face-on since this orientation allows a direct view on the planetary region. The thermal dust reemission of circumstellar disks can be mapped with (sub) millimeter observations and it has been performed successfully for a large number of young stellar objects (e.g., Beckwith et al. 1990). The only observatory, however, which - because of its aspired resolution and sensitivity - might have the capability in the near future to detect features as small as a gap induced by a planet in a young disk, will be *ALMA*. For this reason, we perform radiative transfer simulations in order to obtain images at a frequency of 900 GHz, which marks the planned upper limit of the frequency range to be covered by *ALMA*. This frequency is required for our simulations because it allows to obtain the highest spatial resolution. The trade-off is the relatively high system temperature (~ 1200 K; Guilloteau 2002) which adds a significant amount of noise to the simulated observations. Therefore, long observing times (8h in our simulations) are mandatory. To investigate the resulting maps to be obtained with *ALMA*, we use the *ALMA* simulation software developed by Pety et al. (2001) and chose an observation setup according to the directions and suggestions given by Guilloteau (2002). Furthermore, we introduce a ran-

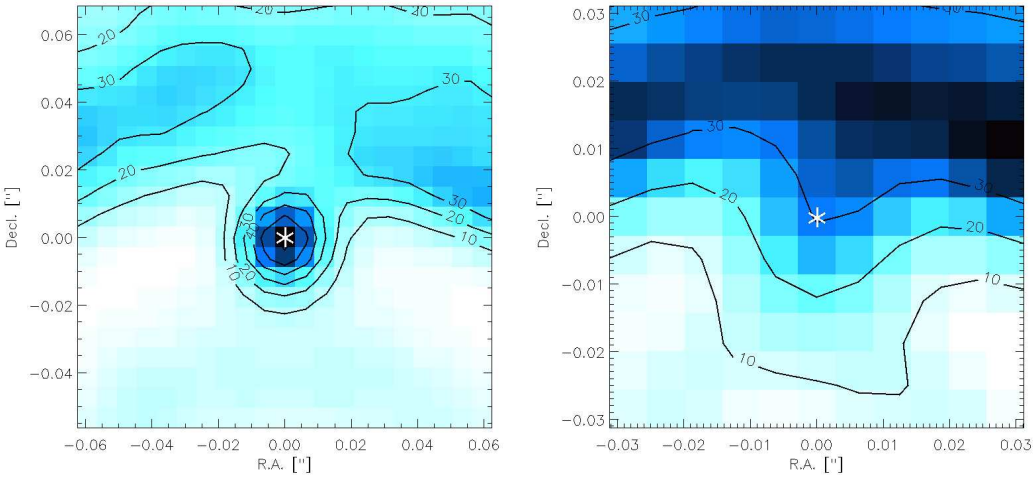

Fig. 4. Simulation of *ALMA* observations with a close-up view of the region around the planet. $M_{\rm P}/M_* = 1\,{\rm M_{jup}}/0.5\,{\rm M_{sun}}$, Comparison of disks, seen at two different distances (left map: 50 pc, right map: 100 pc). The size of the displayed region amounts to 6 AU×6 AU. The asterisk marks the position of the planet. The contour lines mark selected signal-to-noise levels. *[from Wolf & D'Angelo 2005]*

dom pointing error during the observation with a maximum value of 0.6" in each direction, 30° phase noise, and further error sources, such as amplitude errors and "anomalous" refraction (due to the variation of the refractive index of the wet air along the line of sight). The observations are simulated for continuous observations centered on the meridian transit of the object. The object passes the meridian in zenith where an opacity of 0.15 is assumed. The bandwidth amounts to 8 GHz.

Based on these simulations, whose outcomes are shown in Figures 3 and 4, we make the following predictions about the observability of a giant planet in young circumstellar disks:

(1) The resolution of the images to be obtained with *ALMA* will allow detection of the warm dust in the vicinity of the planet only if the object is at a distance of not more than about 50-100 pc. For larger distances, the contrast between the planetary region and the adjacent disk in any of the considered planet/star/disk configurations will be too low to be detectable. However, **the** more pronounced, larger gap can be observed also for objects at larger distances, such as in nearby rich star-forming region (e.g., Taurus; Wolf et al. 2002).
(2) Even at a distance of 50 pc a resolution being high enough to allow a study of the circumplanetary region can be obtained only for those configurations with the planet on a Jupiter-like orbit but not when it is as close as 1 AU to the central star. This is mainly due to the size of the beam ($\sim 0.02''$ for the *ALMA* configuration as described above).
(3) The observation of the emission from the dust in the vicinity of the planet

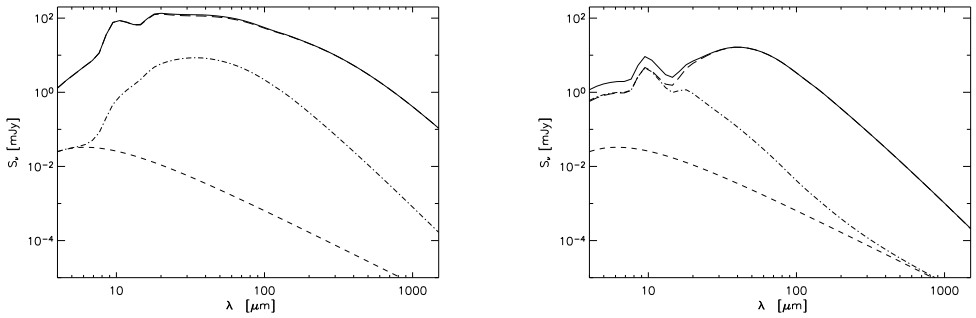

Fig. 5. Spectral energy distribution of protoplanetary disks with embedded planets (simulations). *Left:* $M_{\rm P}/M_* = 1\,{\rm M_{jup}}/0.5\,{\rm M_{sun}}$, $M_{\rm disk} = 10^{-2}\,M_{\rm sun}$ (same model as used for Fig. 4, left column); *Right:* $M_{\rm P}/M_* = 1\,{\rm M_{jup}}/0.5\,{\rm M_{sun}}$, $M_{\rm disk} = 10^{-6}\,M_{\rm sun}$. The planet is located at a distance of 5 AU from the central star. *Solid line*: net SED; *long dashed line*: disk reemission; *short dashed line*: direct (attenuated) and scattered radiation originating from the protoplanet (due to planetary radiation and/or accretion); *dot-dashed line*: (re)emission from the planet and the dust within the sphere with a radius of 0.5 AU centered on the planet. The assumed distance is 140 pc. *[from Wolf & D'Angelo 2005]*

will be possible only in case of the most massive and thus young circumstellar disks ($\sim 10^{-3} - 10^{-2}{\rm M_{sun}}$).

2.2 Influence of the planet on the spectral energy distribution

The contribution of the planet to the net flux at 900 GHz – by direct or scattered radiation and reemission of the heated dust in its vicinity – is $\leq$ 0.4% (depending on the particular model) than that from the small region of the disk considered in our simulations. Furthermore, the planetary radiation significantly affects the dust reemission spectral energy distribution (SED) only in the near to mid-infrared wavelength range (see Fig. 5). However, since this spectral region is influenced also by the warm upper layers of the disk and the inner disk structure, the planetary contribution and thus the temperature / luminosity of the planet cannot be derived from the SED alone.

2.3 Inner cavities in young circumstellar disks?

Observed mid-infrared SEDs of selected disks around T Tauri and debris-type disks show hints of inner cavities (void of small dust grains) such that the inner radius of the disk is apparently much larger than the sublimation radius – at least of selected dust species. Examples among T Tauri disks are GM Aurigae (Koerner et al. 1993, Rice et al. 2003) and TW Hya (Calvet et al. 2002). Two

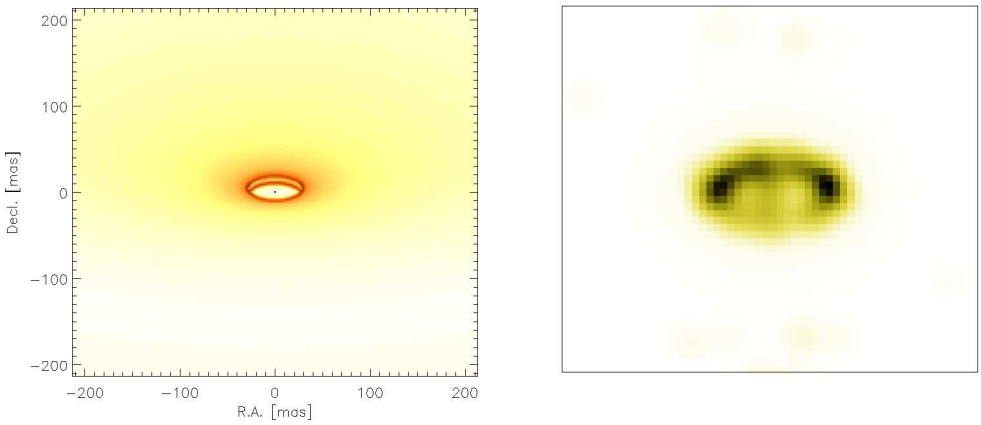

Fig. 6. Simulated 10μm image of the inner region of a T Tauri circumstellar disk with a cleared inner region (radius: 4 AU), seen under an inclination of 60° (assumed distance: 140 pc). *Left:* Original image; *Right:* Reconstructed image (not scaled), based on simulated mid-infrared *VLTI* observations combining 4 Telescope (APreS-MIDI/MATISSE concept study; see e.g., Lopez et al. 2005). *[from Wolf et al. 2005]*

alternatives are discussed to explain these inner "holes": a) dust evolution (mainly grain growth) resulting in a depletion of small grains and b) the influence of a giant planet in the inner region. In Fig. 6 the reconstructed image of a circumstellar disk with an inner hole is shown which could be obtained with the VLTI combining up to 4 Auxiliary Telescopes (Wolf et al. 2005).

3 Debris Disks

3.1 General overview

Debris disks are solar system sized dust disks produced as by-products of collisions between asteroid-like bodies and the activity of comets left over from the planet formation process. In the case of our solar system, the debris of Jupiter-family short-period comets and colliding asteroids represents the dominant source of zodiacal dust located inside the Jupiter orbit. A second belt of dust is located beyond the orbit of Neptune (e.g., Dermott et al. 1992; Liou et al. 1995). Besides the solar system, optical to mid-infrared images of β Pic and AU Mic (e.g., Kalas & Jewitt 1995; Weinberger et al. 2003, Kalas et al. 2004) and (sub)millimeter images of Vega, Fomalhaut, ϵ Eri, and β Pic (Holland et al. 1998; Greaves et al. 1998, Liseau et al. 2003) have revealed spatially resolved debris disks which were first inferred from observations of infrared flux excesses above photospheric values with *IRAS*. Based on stud-

ies with *ISO*, the disk fraction is thought to decrease significantly with age, amounting to much less than 10% for stars with ages $\geq$ 1Gyr (e.g., Spangler et al. 2001; see also Habing et al. 2001; Greaves et al. 2004; Dominik & Decin 2003). Planetary debris disks are assumed to represent the almost final stage of the circumstellar disk evolution process, i.e., they are the evolutionary products of ongoing or completed planet formation.

In contrast to optically thick young circumstellar disks around Herbig Ae/Be and T Tauri stars with spatial structures dominated by gas dynamics, the much lower optical depth and lower gas-to-dust mass ratio in debris disks (Zuckerman et al. 1995; Dent et al. 1995; Artymowicz 1997; Liseau & Artymowicz 1998; Greaves et al. 2000a; Lecavelier et al. 2001) let the stellar radiation – in addition to gravity – be responsible for the disk structure. Besides, fragmentation becomes a typical outcome of particle collisions, because relative velocities of grains are no longer damped by gas. The Poynting-Robertson (P-R) effect, radiation pressure, collisions, and gravitational stirring by embedded planets are all important in determining the dust population and disk structure (Liou & Zook 1999; Grady et al. 2000; Moro-Martín & Malhotra 2002).

Since the mass of small grains in debris disks and therefore the thermal dust reemission from these disks are much smaller than in case of T Tauri disks, only a very limited sample of observations existed in the recent past, as IRAS and ISO could only probe the brightest and closest system. However, because of the unprecedented sensitivity of the mid-infrared detectors aboard the *Spitzer Space Telescope* there has been a substantial increase in the total number of detected debris disks. As an example, the A-Star and FGK GTO Surveys and the FEPS Legacy Survey (cf. Meyer et al. 2004) are allowing to extend the search for disks around stars to greater distances and more tenuous disks, achieving detections rates adequate to establish disk frequency and properties on a sound statistical basis (e.g., Rieke et al. 2005; Bryden et al. 2005; Beichman et al. 2005).

In the simplest model of debris disks, their structure is controlled by gravity, radiation pressure, and P-R drag. In a collisionless system without sources and sinks and with grains in circular orbits, the radial density distribution $\rho(r)$ decreases as $1/r$ due to P-R drag (e.g., Briggs 1962). This "classical solution" approximately represents the overall distribution of dust in the solar system (e.g., Ishimoto 2000). Another simply-structured debris disk would be a cloud of grains moving outward from the centre in hyperbolic trajectories. This solution, which applies to so-called β-meteoroids in the interplanetary space is described by $\rho(r) \propto r^{-2}$ (e.g., Lecavelier des Etangs et al. 1998; Ishimoto 2000). However, as for instance Gor'kavyi et al. (1997) pointed out, there exist several effects that may change the distribution considerably, including resonance effects with planets, gravitational encounters with planets

which occur in the form of elastic gravitational scattering, mutual collisions of particles, evaporation of dust grains, and existence of sources of dust with highly eccentric orbits (such as the Encke comet in the case of the solar system; e.g., Whipple 1976, Sykes 1988, Epifani et al. 2001). The resulting density distribution is in most cases no longer described by a single power-law, but depends strongly on the properties (mainly the orbits and masses of planets and dust sources) of each particular disk/planetary system. In the case of β Pic, visible observations of the scattered starlight and mid-infrared images show a decrease of the mid-plane number density profile with increasing distance from the central star (Artymowicz et al. 1989; Kalas & Jewitt 1995), possibly indicating that most of the dust sources are located in the inner disk.

Although debris disks represent a rich source of information about the formation and evolution of planetary systems, they also impose problems on the observations of exoplanetary systems. First, zodiacal light of our own solar system has a potential serious impact on the ability of space-born observations to detect and study their targets. It is attributed to the scattering of sunlight in the UV to near-IR, and – important for mid-IR missions such as *DARWIN* (e.g., Fridlund 2000) – the thermal dust reemission in the mid to far-IR. At infrared wavelengths from approximatelly 1μm, the signal from the zodiacal light is a major contributor to the diffuse sky brightness and dominates the mid-IR sky in nearly all directions, except for very low galactic latitudes (Gurfil et al. 2002). Based on measurements obtained with the *COBE* satellite, Fixsen & Dwek (2002) derived an annually averaged spectrum of the zodiacal cloud in the 10-100μm wavelength range. The spectrum exhibits a break at $\sim$150μm that indicates a knee in the dust size distribution at a radius of about 30μm (see Fig. 7).

Second, the exozodiacal dust disk around a target star, even at solar level, will likely be the dominant signal originating from the extrasolar system. In the case of a solar system twin, its overall flux over the first 5 AU is about 400 times larger than the emission of the Earth at 10μm. Although the factor reduces to a few tens after partial rejection by usage of a nulling interferometer, one still has to make sure that the exo-zodiacal signature will not mimic planetary signals such as would be the case if the disk is significantly clumpy (as almost always found in the outer regions of debris disk – e.g., Holland et al. 1998; Greaves et al. 1998; Holland et al. 2003). If the origin of this clumpiness is in perturbations of planets, then detecting clumps can help to pinpoint those planets (e.g., Wyatt 2003). In this context one has to be aware that collisionally regenerated debris disks are also intrinsically clumpy because dust created by collisions between large planetesimals starts out in a clumpy dust distribution (Wyatt & Dent 2002).

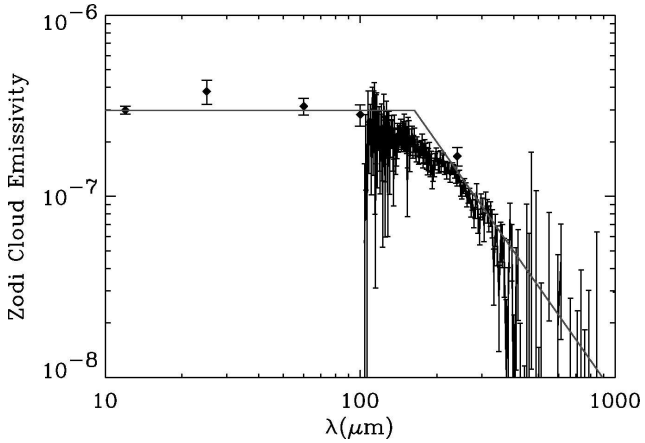

Fig. 7. The annually averaged spectrum of the zodiacal light, normalized to that of a 240 K blackbody. Diamonds represent *DIRBE* data, and the solid error bars represent the *FIRAS* spectrum. At wavelengths below $\sim$150μm, the zodiacal spectrum is that of a graybody with an optical depth of $\sim 3\times10^{-7}$ (similar to the value 10^{-7} quoted by Leinert 1996). At longer wavelengths the dust emissivity falls off as λ^{-2}, as shown by the solid line. *[from Fixsen & Dwek 2002]*

3.2 Structure of debris disks with embedded planets

The high-resolution images of debris disks in scattered light in the optical/near-IR and in thermal emission at mid-IR to millimeter wavelengths show the presence of density structure, such as rings, gaps, arcs, warps, offset asymmetries and clumps of dust (e.g., Greaves et al. 1998; Schneider et al. 1999; Wilner et al. 2002; Holland et al. 1998, 2003; Koerner et al. 2001). In evolved, optically thin debris disks some of these features are likely to be the result of gravitational perturbations by one or more massive planets on the dust disk. There are several mechanisms by which giant planets can sculpt the disks: (a) capture of dust in mean motion resonances (MMRs) with the planet, as the dust particles drift toward the central star due to P-R drag; (b) gravitational scattering of dust particles by the planet; (c) resonance capture of dust-producing planetesimals due to planet migration; and (d) secular (long-term) planetary perturbations. The resulting characteristic density patterns are expected to provide the strongest indirect hints on the existence of planets embedded in these disks (see e.g., Liou & Zook 1999; Wyatt et al. 1999; Ozernoy et al. 2000; Moro-Martín & Malhotra 2002, 2003, 2005; Wilner et al. 2002; Quillen & Thorndike 2002; **Sremčević et al. 2002**; Kuchner & Holman 2003).

Resonant trapping takes place when the orbital period of the planet is $(p+q)/p$ times that of the particle, where p and q are integers, $p>0$ and $p+q\geqslant1$. Taking into account radiation pressure force, $a/a_p=[(p+q)/p]^{2/3}\times(1\text{-}\beta)^{1/3}$, where a and a_p are the semimajor axis of the orbit of the particle and of the planet repectively and β is the ratio of the radiation pressure force to the gravita-

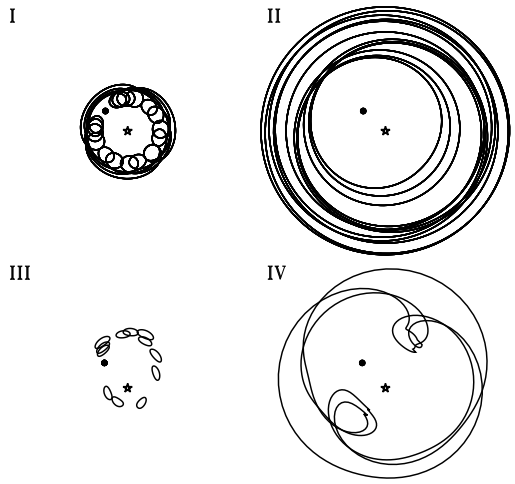

Fig. 8. Four basic resonant structures in debris disks: (I) low-mass planet on a low-eccentricity orbit, (II) high-mass planet on a low-eccentricity orbit, (III) low-mass planet on a moderate-eccentricity orbit, and (IV) high-mass planet on a moderate-eccentricity orbit. *[from Kuchner & Holman 2003]*

tional force. Each resonance has a libration width Δa, that depends on the particle eccentricity and the planet mass, in which resonant orbits are stable, while resonance overlapping makes the region close to the planet chaotic. When trapped in outer MMRs (q>0), the dust particle receives energy from the inner planet, balancing the energy loss due to P-R drag. This makes the lifetime of particles trapped in outer MMRs longer than in inner MMRs, with the former dominating the disk structure.

Kuchner & Holman (2003) pointed out that four basic resonant structures probably represent the range of high-contrast resonant structures a planet with eccentricity $\lesssim 0.6$ can create in a disk of dust released on low eccentric orbits: (i) A ring with a gap at the location of the planet, (ii) a smooth ring, (iii) a clumpy eccentric ring, and (iv) an offset ring plus a pair of clumps. The appearance / dominance of one of these structures mainly depends on the mass of the planet and the eccentricity of its orbit (Fig. 8).

The dust disk produced by the Kuiper Belt objects in our own Solar System is an example of a debris disk with embedded massive planets in circular orbits. In the Solar System, the planet dominating the trapping of particles in MMRs is the outermost massive planet Neptune. Dynamical models show that the dust disk density is enhanced in a ring-like structure between 35–50 AU, with some azimuthal variation due to the trapping into MMRs and the fact

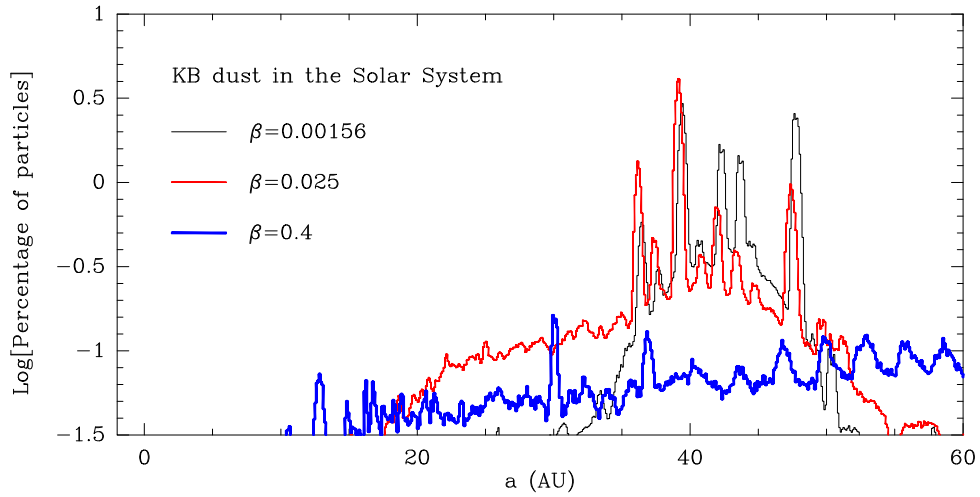

Fig. 9. Semimajor-axis distribution of Kuiper Belt dust particles, showing the the percentage of particles (in log scale) found at a particular semimajor-axis. The different colors and line weights represent different particle sizes or β-values with the black (thin), red (medium) and blue (heavy) lines corresponding to β-values of 0.00156, 0.025 and 0.4, respectively (which for astronomical silicates would correspond to particle sizes of 135, 8.8, and 0.7 μm, respectively). *[from Moro-Martín, Wolf & Malhotra, in prep.]*

that trapped particles tend to avoid the resonance planet, creating a minimun density at Neptune's position. The effect of trapping into MMRs can clearly be seen in the "equilibrium" semimajor axis distributions shown in Fig. 9 and the disk surface density distributions shown in Fig. 10 (from Moro-Martín & Malhotra 2002). Both figures show how the dust disk structure is more pronounced for larger particle sizes (smaller β) as the trapping in MMRs is more efficient when the drag forces are small.

One of the most prominent features in Fig. 9 and Fig. 10 is the strong depletion of dust inside 10 AU due to gravitational scattering of dust particles by Jupiter and Saturn. Moro-Martín & Malhotra (2005) explored how this effect depends on planet mass, semimajor-axis, eccentricity, and particle size. They found that planets with masses of 3–10 M_{Jup} located between 1–30 AU eject >90% of the particles that go past their orbits, while a 1 M_{Jup} planet at 30 AU ejects > 80% of the particles, and about 50%–90% if located at 1 AU, with these results being valid for particles with β-values between 0.00156 and 0.4 (see Fig. 11). This results in a lower dust number density within the planet's orbit, as the dust grains drifting inward due to the P-R effect are likely to be scattered into larger orbits.

Inner cleared regions have been found in several debris disks: β Pic (inner

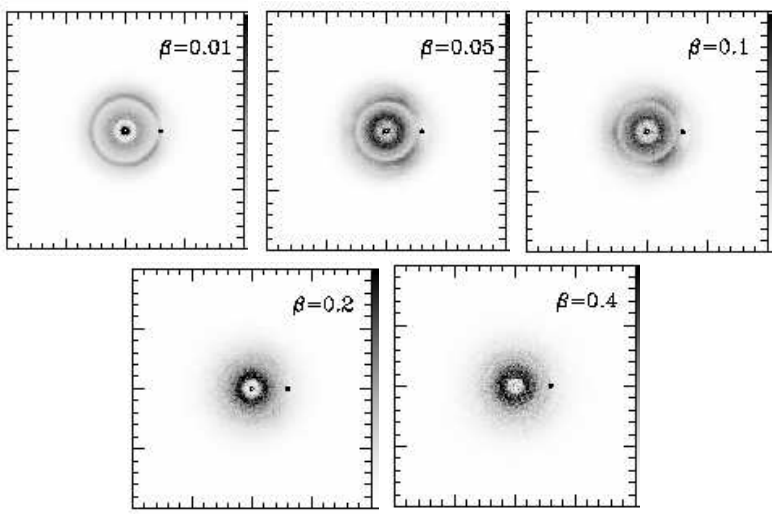

Fig. 10. Number density distribution of Kuiper Belt dust grains of different particle sizes, corresponding to different β-values. The dot to the right of the centre indicates the position of Neptune. As in the previous figure, the trapping of particles in the exterior MMRs with Neptune and the depletion of particles in the inner 10 AU due to gravitational scattering with Jupiter and Saturn are the most prominent features. *[from Moro-Martín & Malhotra 2002]*

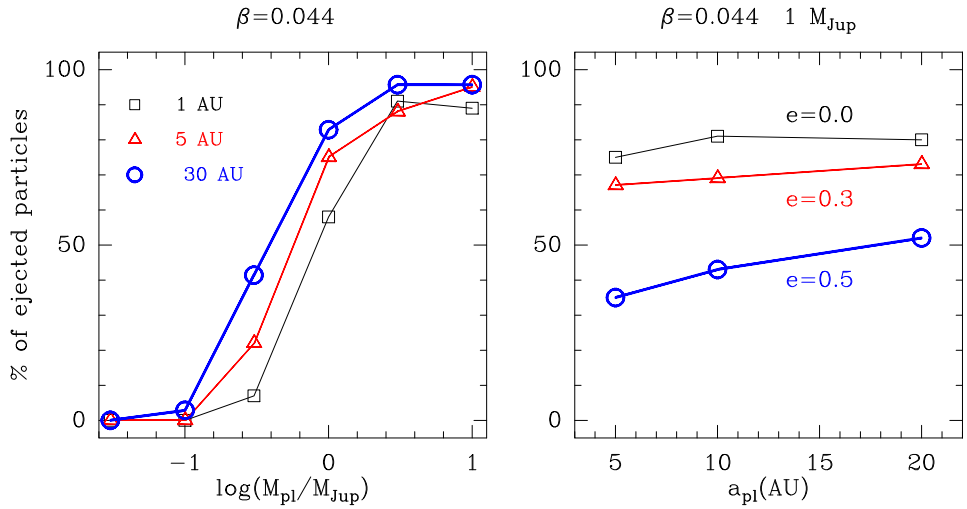

Fig. 11. (Left) Percentage of ejected particles (with β=0.044) as a function of planet mass for systems consisting on an outer belt of dust-producing planetesimals and a single massive planet in a circular orbit. The different colors and line weights correspond to different planet semimajor-axis. (Right) Percentage of ejected particles as a function of planet semimajor axis. The different colors and line weights correspond to different planet eccentricities. *[from Moro-Martín & Malhotra 2005]*

radius: 20 AU), HR 4796A (30-50 AU), ϵ Eri (50 AU), Vega (80 AU), and Fomalhaut (125 AU) – e.g., Dent et al. 2000; Greaves et al. 2000b; Wilner et al. 2002; Holland et al. 2003. These cavities may be created by gravitational scattering with an inner planet.

Krivov et al. (2000) pointed out that the P-R effect can be ignored in disks with optical depths smaller than about 10^{-4} (see also Artymowicz 1997). For Solar System analogs, fainter than the disks observed to date and that telescopes like *ALMA* **and *DARWIN*** will be able to detect, P-R drag dominates the dynamics of the dust particles and therefore, in that density regime, gravitational scattering with massive planets is likely responsible for the creation of inner cavities (if observed).

Another two prominent examples for which the possible influence of a planet on the disk structure has been discussed are the debris disks around Vega and β Pictoris. The first shows two dominating emission peaks / density enhancements in spatially resolved submillimeter maps (Holland et al. 1998, Wilner et al. 2002). However, Su et al. (2005) did not confirm the existence of these structures, but found a circular, smooth brightness distribution without indications of clumpiness in high spatial resolution mid- and far-infrared images obtained with MIPS/Spitzer. The β Pictoris disk is seen nearly edge-on and extends to at least a distance of 100 AU from the central star (Zuckerman & Becklin 1993, Holland et al. 1998, Dent et al. 2000, Pantin, Lagage, & Artymowicz 1997). The Northeast and Southwest extensions of the dust disk have been found to be asymmetric in scattered light as well as in thermal emission. This warp is assumed to be caused by a giant planet on an inclined orbit that gravitationally perturbs the dust disk (Augereau et al. 2001; Mouillet et al. 1997; see also Lubow & Ogilvie 2001).

3.3 Signatures of planets in spatially unresolved debris disks

Besides high-resolution imaging of debris disks, mid-infrared spectroscopy is a valuable tool to deduce the existence of an inner gap, since the deficiency of hot dust in the stellar vicinity causes a decrease of the mid-infrared flux compared to an undisturbed disk. With increasing gap size the emission spectrum is shifted toward longer wavelengths and the mid-infrared flux is reduced (see Fig. 12). Detailed studies of the influence of planets on the SED of debris disks have been performed by Wolf & Hillenbrand (2003) and Moro-Martín, Wolf, & Malhotra (2005). Moro-Martín et al. (2005), carried out a study on how the dust density structure carved by massive planets affected the shape of the disk SED. The disk SED depends on the grain properties (chemical composition, density, and size distribution), the mass, and location of the per-

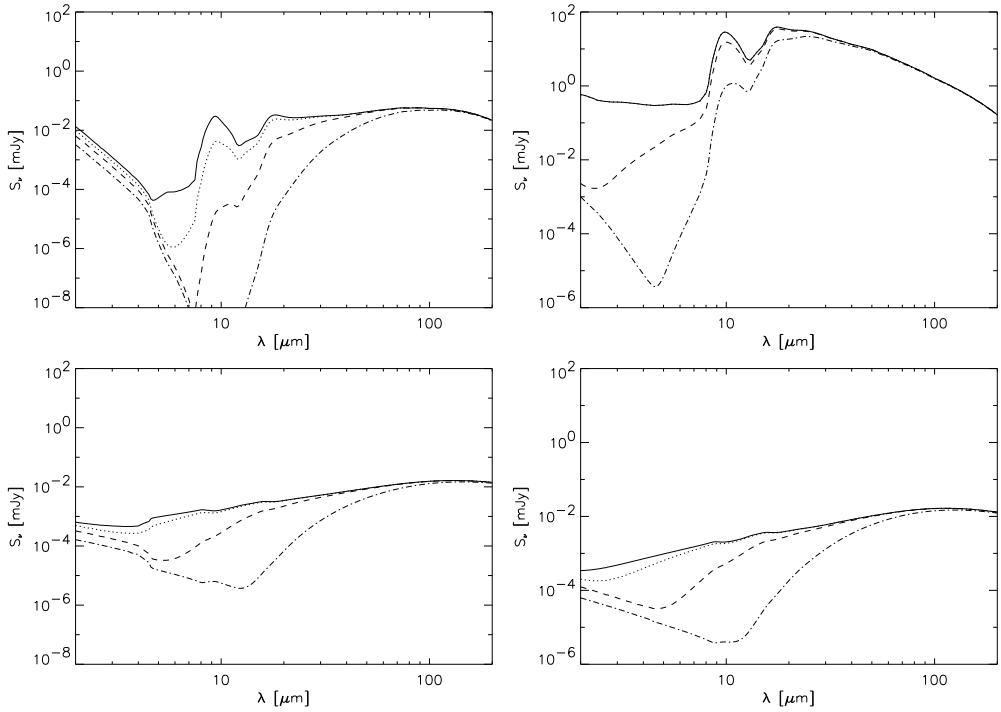

Fig. 12. Influence of an inner gap on the SED of a debris disk. Inner disk radius: dust sublimation radius (solid line), 0.1 AU (dotted), 1 AU (dashed), and 10 AU (dash-dotted). Left / Right column: Fe-poor Silicate ($MgSiO_3$) / Fe-rich Silicate (Olivine, $MgFeSiO_4$). *Top:* $a = 0.1\mu$m, *Bottom:* $a = 1$mm. Disk mass: $10^{-10}M_{sun}$. The central star has a solar-type SED (we use the solar SED published by Labs & Neckel 1968, extended by a blackbody SED beyond 151 μm). The distance to the system is assumed to be 50 pc. *[from Wolf & Hillenbrand 2003]*

turbing planet. They found that (1) the SED of a debris disk with embedded giant planets is fundamentally different from that of a disk without planets, the former showing a significant decrease of the near/mid-IR flux due to the clearing of dust inside the planet's orbit. (2) The SED is particularly sensitive to the location of the planet, i.e. to the area interior to the planet's orbit that is depleted in dust (see Fig. 13, from Moro-Martín et al. 2005). (3) There exist some degeneracies that can complicate the interpretation of the SED in terms of planet location. For example, the SED of a dust disk dominated by weakly absorbing grains (e.g., Fe-poor silicates) has its minimum at wavelengths longer than those of a disk dominated by strongly absorbing grains (e.g., carbonaceous and Fe-rich silicate). Because the SED minimum also shifts to longer wavelengths when the gap radius increases (owing to a decrease in the mean temperature of the disk), there might be a degeneracy between the dust grain chemical composition and the semimajor axis of the planet clearing the gap (see Fig. 14, from Moro-Martín et al. 2005).

The *Spitzer* space telescope is carrying out spectrophotometric observations of hundreds of circumstellar disks most of which are spatially unresolved. The

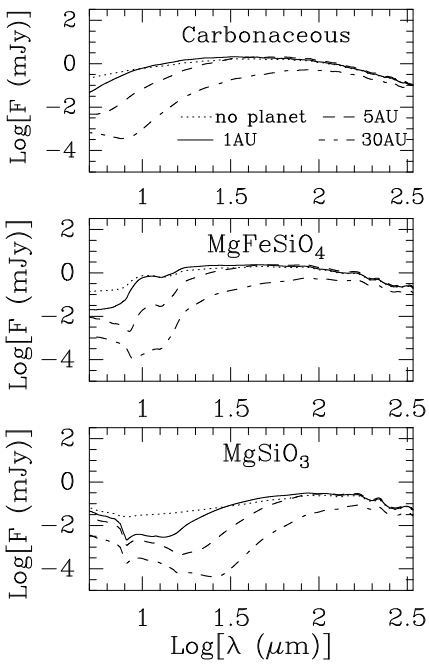

Fig. 13. SEDs of dust disks in the presence of different planetary configurations [*solid*: $3M_{Jup}$ at 1 AU; *dashed*: $3M_{Jup}$ at 5 AU; *dashed − dotted*: $3M_{Jup}$ at 30 AU; *dotted*: system without planets]. Results are shown for three grain chemical compositions (indicated in each panel), and particle size distribution given by $n(b)db = n_0 b^{-q}$ with q=3.0. In all cases the system is at a distance of 50 pc and has a total disk mass of 10^{-10} M_{sun}. *[from Moro-Martín, Wolf & Malhotra 2005]*

study of these SEDs can help us diagnose the **radial** distribution of dust, allowing us to identify targets where the dynamical imprints of embedded giant planets may be present (e.g., Kim et al. 2005; Beichman et al. 2005). But because the SEDs are **degenerate**, to unambigously constrain the planet location we need to obtain high resolution images able to spatially resolve the disk. In the future, telescopes like *ALMA*, *SAFIR*[2], *TPF*[3], *DARWIN* and *JWST*[4] will be able to image the dust in planetary systems analogous to our own. If observed from afar, the Kuiper Belt dust disk would be the brightest extended feature in the solar system, and its structure, if spatially resolved, could be recognized as harboring at least two giant planets: an inner planet (Jupiter plus Saturn) and outer planet (Neptune) (Liou et al. 1996; Moro-Martín & Malhotra 2002). The goal is that high-resolution, high-sensitivity imaging of debris disks around other stars will help us learn about the frequency and diversity of planetary systems, helping us place our solar system into context.

[2] Single Aperture Far Infrared Telescope
[3] Terrestrial Planet Finder
[4] James Webb Space Telescope

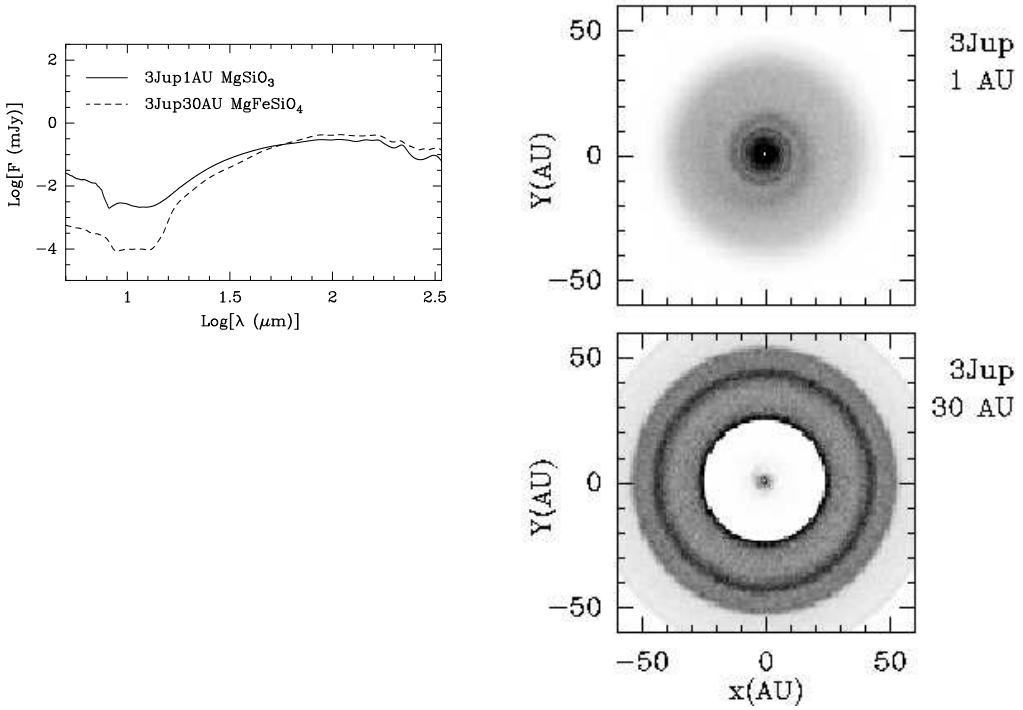

Fig. 14. *[Left]* Possible degeneracy between the grain chemical composition and the location of the planet clearing the gap. *Solid line*: SED of dust disk composed of $MgSiO_3$ grains with a $3M_{Jup}$ planet at 1 AU; *dashed line*: same for $MgFeSiO_4$ grains with a $3M_{Jup}$ planet at 30 AU. In both cases q=2.5. *[Right]* Brightness density distributions at 70 μm (assuming graybody emission from 12 μm grains) expected from a disk with a $3M_{Jup}$ planet at 1 AU (top) and 30 AU (bottom), respectively (shown in arbitrary units). High resolution images are needed to solve the degeneracy. *[from Moro-Martín, Wolf & Malhotra 2005]*

4 Summary

Numerical simulations convincingly demonstrate that high-resolution imaging performed with instruments / telescopes that will become available in the near future will allow detection of planets in circumstellar disks. However, scattering of stellar light and thermal emission by small grains – in the case of optically thick disks seen at high inclination also absorption – will make direct planet detection via imaging hardly feasible. But planets cause large-scale perturbations in the disks which will be observable with observatories like the *Stratospheric Observatory For Infrared Astronomy* (*SOFIA*), the *James Webb Space Telescope* (*JWST*), but also ground-based observatories / interferometers, such as *ALMA* or the *VLTI* by spatially resolved mapping of the dust reemission. The particular type of perturbation depends on the evolutionary stage of the disk. **The most prominent** signatures of planets embedded in disks are gaps and circumplanetary accretion disks in the case of young disks and characteristic asymmetric density patterns in debris disks. **Further** signatures are, for instance, spiral structures in young disks or warps due to planets on inclined orbits.

Acknowledgement

S.W. is supported by the German Research Foundation (DFG) through the Emmy Noether grant WO 857/2-1. A.M.M. is under contract with the Jet Propulsion Laboratory (JPL) funded by NASA through the Michelson Fellowship Program. JPL is managed for NASA by the California Institute of Technology. AMM is also supported by the Lyman Spitzer Fellowship at Princeton University. G.D. is grateful to the Leverhulme Trust for support under a UKAFF (UK Astrophysical Fluids Facility) Fellowship.

References

[1] Adams, F.C., Lada, C.J., Shu, F.H. 1987, ApJ, 312, 788
[2] Artymowicz, P., Annu. Rev. Earth Planet. Sci. 1997, 25, 175
[3] Artymowicz, P., Burrows, C., Paresce, F. 1989, ApJ, 337, 494
[4] Augereau, J.C., Nelson, R.P., Lagrange, A.M., Papaloizou, J.C.B., Mouillet, D. 2001, A&A, 370, 447
[5] Bate, M.R., Lubow, S.H., Ogilvie, G.I., Miller, K.A. 2003, MNRAS, 341, 213
[6] Beckwith, S.V.W., Sargent, A.I., Chini, R.S., Guesten, R. 1990, AJ, 99, 924
[7] Beichman, C.A, Bryden, G., Rieke, G.H., Stansberry, J.A., Trilling, D.E., Stapelfeldt, K.R., Werner, M.W., Engelbracht, C.W., Blaylock, M., Gordon, K.D., Chen, C.H., Su, K.Y.L., Hines, D.C. 2005, ApJ, 622, 1160

[8] Briggs, R.E. 1962, AJ, 67, 710
[9] Bryden, G., Beichman, C.A., Trilling, D.E. et al. 2005, ApJ, in press
[10] Bryden, G., Chen, X., Lin, D.N.C., Nelson, R.P., Papaloizou, J.C.B. 1999, ApJ, 514, 344
[11] Burrows, A., Marley, M., Hubbard, W.B., Lunine, J.I., Guillot, T., et al. 1997, ApJ, 491, 856
[12] D'Angelo, G., Henning, Th., Kley, W. 2002, A&A, 385, 647
[13] D'Angelo, G., Kley, W., Henning, Th. 2003, ApJ, 586, 540
[14] Dent, W.R.F., Greaves, J.S., Mannings, V., Coulson, I.M., Walther, D.M. 1995, MNRAS, 277, L25
[15] Dent, W.R.F., Walker, H.J., Holland, W.S., Greaves, J.S. 2000, MNRAS, 314, 702
[16] Dermott, S.F., Durda, D.D., Gustafson, B.A., Jayaraman, S., Xu, Y.L., Gomes, R.S., Nicholson, P.D. 1992, in Asteroids, Comets, Meteors, A.W. Harris & E. Bowell (eds.), 153
[17] Dominik, C., Decin, G. 2003, ApJ, 598, 626
[18] Epifani, E., Colangeli, L., Fulle, M., Brucato, J.R., Bussoletti, E., de Sanctis, M. C., Mennella, V., Palomba, E., Palumbo, P., Rotundi, A. 2001, Icarus, 149, 339, 2001
[19] Fixsen, D.J., Dwek, E. 2002, ApJ, 578, 1009
[20] Fridlund, C.V.M. 2000, "Darwin - The Infrared Space Interferometry Mission", ESA Bulletin, 103, 20
[21] Goldreich, P., Ward W.R. 1973, ApJ, 183, 1051
[22] Gor'kavyi, N.N., Ozernoy, L.M., Mather, J.C., Taidakova, T. 1997, ApJ, 488, 268
[23] Grady, C.A., Sitko, M.L., Russell, R.W., Lynch, D.K., Hanner, M.S., Perez, M.R., Bjorkman, K.S., de Winter, D. 2000, In Protostars and Planets IV, V. Mannings, A.P. Boss, S.S. Russell (eds.), University of Arizona Press, p. 613
[24] Greaves, J.S., Coulson, I.M., Holland, W.S. 2000a, MNRAS, 312, L1
[25] Greaves, J.S., Holland, W.S., Jayawardhana, R., Wyatt, M.C., Dent, W.R.F. 2004, MNRAS, 348, 1097
[26] Greaves, J.S., Holland, W.S., Moriarty-Schieven, G., Jenness, T., Dent, W.R.F., Zuckerman, B., McCarthy, C., Webb, R.A., Butner, H.M., Gear, W.K., Walker, H.J. 1998, ApJ, 506, L133
[27] Greaves, J.S., Mannings, V., Holland, W.S. 2000b, Icarus, 143, 155
[28] Guilloteau, S. 2002, ALMA Memo, 393
[29] Gurfil, P., Kasdin, J., Arrell, R., Seager, S., Nissanke, S.M. 2002, ApJ, 567, 1250
[30] Habing, H.J., Dominik, C., Jourdain de Muizon, M., Laureijs, R.J., Kessler, M.F., Leech, K., Metcalfe, L., Salama, A., Siebenmorgen, R., Trams, N., Bouchet, P. 2001, A&A, 365, 545
[31] Holland, W.S., Greaves, J.S., Dent, W.R.F., Wyatt, M.C., Zuckerman, B., Webb, R.A., McCarthy, C., Coulson, I.M., Robson, E.I., Gear, W.K. 2003, ApJ, 582, 1141

[32] Holland, W.S., Greaves, J.S., Zuckerman, B., Webb, R.A., McCarthy, C., Coulson, I.M., Walther, D.M., Dent, W.R.F., Gear, W.K., Robson, I. 1998, Nature, 392, 788
[33] Hubbard, W.B., Burrows, A., Lunine, J.I. 2002, ARAA, 40, 103
[34] Ishimoto, H. 2000, A&A, 362, 1158
[35] Kalas, P., Jewitt, D. 1995, ApJ, 110, 794
[36] Kalas, P., Liu, M.C., Matthews, B.C. 2004, Science, 303, 1990
[37] Kim, J.S, Dean, D.C., Backman, D.E. et al. 2005, ApJ, 632, 659
[38] Kley, W. 1999, MNRAS, 303, 696
[39] Koerner, D.W., Sargent, A.I., Ostroff, N.A. 2001, ApJ, 560, L181
[40] **Krivov, A.V., Mann, I., Krivova, N.A. 2000, A&A, 362, 1127**
[41] Kuchner, M.J., Holman, M.J. 2003, ApJ, 588, 110
[42] Labs, D., Neckel, H. 1968, ZA, 69, 1
[43] Lecavelier des Etangs, A., Vidal-Madjar, A., Ferlet, R. 1998, A&A, 339, 477
[44] Lecavelier des Etangs, A., Vidal-Madjar, A., Roberge, A., Feldman, P.D., Deleuil, M., Andr, M., Blair, W.P., Bouret, J.-C., Dsert, J.-M., Ferlet, R., Friedman, S., Hbrard, G., Lemoine, M., Moos, H. W. 2001, Nature, 412, 706
[45] Liou, J.-C., Dermott, S.F., Xu, Y.-L. 1995, Planet. Space Sci., 43, 717
[46] Liou, J.C., Zook, H.A., Dermott, S.F. 1996, Icarus, 124, 429
[47] Liou, J.C., Zook, H.A. 1999, AJ, 118, 580
[48] Liseau, R., Artymowicz, P. 1998, A&A, 334, 935
[49] Lissauer, J.J. 1993, ARA&A, 31, 129
[50] Lopez, B., Wolf, S., Dugue, M., Graser, U., Mathias, Ph., et al. 2005, "Aperture Synthesis in the MID-Infrared (10μm) with the VLTI", In Proceedings of "The Power of Optical/Infrared Interferometry: Recent Scientific Results and Second Generation VLT Instrumentation", Garching, Germany, in press
[51] Lubow, S.H., Ogilvie, G.I. 2001, ApJ, 560, 997
[52] Lubow, S.H., Seibert, M., Artymowicz, P. 1999, ApJ, 526, 1001
[53] Marcy, G., Butler, R.P., Fischer, D.,Vogt, S., Wright, J.T., Tinney, C.G., Jones, H.R.A. 2005, Progress of Theoretical Physics Supplement, 158, 24
[54] Meyer, M.R., Hillenbrand, L.A., Backman, D.E., Beckwith, S.V.W., Bouwman, J., Brooke, T.J., Carpenter, J.M., Cohen, M., Gorti, U., Henning, Th., Hines, D.C., Hollenbach, D., Kim, J.S., Lunine, J., Malhotra, R., Mamajek, E.E., Metchev, S., Moro-Martín, A., Morris, P., Najita, J., Padgett, D.L., Rodmann, J., Silverstone, M.D., Soderblom, D.R., Stauffer, J.R., Stobie, E.B., Strom, S.E., Watson, D.M., Weidenschilling, S.J., Wolf, S., Young, E., Engelbracht, C.W., Gordon, K.D., Misselt, K., Morrison, J., Muzerolle, J., Su, K. 2004, ApJSS, 154, 422
[55] Moro-Martín, A., Malhotra, R. 2002, AJ, 124, 2305
[56] Moro-Martín, A., Malhotra, R. 2003, AJ, 125, 2255
[57] Moro-Martín, A., Malhotra, R. 2005, ApJ, 633, 1150
[58] Moro-Martín, A., Wolf, S., Malhotra, R. 2005, ApJ, 621, 1079

[59] Moro-Martín, A., Wolf, S., Malhotra, R. 2006, in prep.
[60] Mouillet, D., Larwood, J.D., Papaloizou, J.C.B., Lagrange, A.M. 1997, MNRAS, 292, 896
[61] Nelson, R.P., Papaloizou, J.C.B. 2003, MNRAS, 339, 993
[62] Ozernoy, L.M., Gorkavyi, N.N., Mather, J.C., Taidakova, T.A. 2000, ApJ, 537, 147
[63] Pantin, E., Lagage, P.O., Artymowicz, P. 1997, ApJ, 327, 1123
[64] Pety, J., Gueth, F., Guilloteau, S. 2001, ALMA Memo.398
[65] Pollack, J.B., Hubickyj, O., Bodenheimer, P., Lissauer, J.J., Podolak, M., Greenzweig, Y. 1996, Icarus, 124, 62
[66] Rieke, G.H., Su, K.Y.L., Stansberry, J.A. et al. 2005, ApJ, 620, 1010
[67] Schneider, G., Smith, B.A., Becklin, E.E et al. 1999, ApJ, 513, L127.
[68] Spangler, C., Sargent, A.I., Silverstone, M.D., Becklin, E.E., Zuckerman, B. 2001, ApJ, 555, 932
[69] **Sremčević, M., Spahn, F., Duschl, W.J. 2002, MNRAS, 337, 1139**
[70] **Su, K.Y.L., Rieke, G.H., Misselt, K.A., Stansberry, J.A., Moro-Martin, A., et al. 2005, ApJ, 628, 487**
[71] Sykes, M.V. 1988, ApJ, 334, L55
[72] Quillen, A.C., Thorndike, S. 2002, ApJL, 2002, 578, 149
[73] Weidenschilling, S. 1997, Icarus, 127, 290
[74] Weinberger, A.J., Becklin, E.E., Zuckerman, B. 2003, ApJ, 584, L33
[75] Whipple, F.L. 1976, In: "Interplanetary dust and zodiacal light", Berlin and New York, Springer-Verlag 1976, p. 403
[76] Wilner, D.J, Holman, M.J., Kuchner, M.J., Ho, P.T.P. 2002, ApJ, 569, L115
[77] Winters, W.F., Balbus, S.A., Hawley, J.F. 2003, ApJ, 589, 543
[78] Wolf, S. 2003, Comp. Phys. Comm., 150, 99
[79] Wolf, S., D'Angelo, G. 2005, ApJ, 619, 1114
[80] Wolf, S., Gueth, F., Henning, Th., Kley, W. 2002, ApJ, 566, L97
[81] Wolf, S., Henning, Th., Stecklum B. 1999, A&A, 349, 839
[82] Wolf, S., Hillenbrand, L.A. 2003, ApJ, 596, 603
[83] Wolf, S., Lopez, B., Augereau, J.-Ch., Berruyer, N., Chesneau, O., et al. 2005, "APreS-MIDI Science Case Study", subm. to ESO
[84] Wyatt, M.C. 2003, ApJ, 598, 1321
[85] Wyatt, M.C., Dent, W.R.F. 2002, MNRAS, 334, 589
[86] Wyatt, M.C., Dermott, S.F., Telesco, C.M. 1999, ApJ, 527, 918
[87] Youdin, A.N., Shu, F.H. 2002, ApJ, 580, 494
[88] Zuckerman, B., Becklin, E.E. 1993, ApJ, 414, 793
[89] Zuckerman, B., Forveille, T., Kastner, J.H. 1995, Nature, 373, 494